Structure-Based Design of a Novel Series of Nonpeptide Ligands That Bind to the pp60[src] SH2 Domain

Elizabeth A. Lunney,* Kimberly S. Para,[†] J. Ronald Rubin,[‡] Christine Humblet, James H. Fergus,[§] James S. Marks,[§] and Tomi K. Sawyer

Contribution from the Departments of Chemistry and Biochemistry, Parke-Davis Pharmaceutical Research, Division of Warner-Lambert Company, 2800 Plymouth Road, Ann Arbor, Michigan 48106

Received June 2, 1997[⊗]

Abstract: The SH2 domain of pp60[c−src] (Src), a nonreceptor tyrosine kinase, facilitates signal transduction in a number of cell types through binding to cognate phosphorylated protein sequences. Phosphotyrosine-containing peptides have been shown to bind to the Src SH2 domain with micromolar affinity. Guided by the X-ray crystal structure of a phosphorylated peptide bound to the Src SH2 domain, we have designed a *de novo* series of small molecule ligands that bind with affinity comparable to the parent phosphopeptide. An X-ray crystal structure of the Src SH2 domain bound with a nonpeptide analog from this series verifies interactions targeted in the molecular design. However, a unique mode of binding has been revealed for the P-site phenyl phosphate group of the nonpeptide that differs from that observed for the phosphotyrosine side chain in peptide ligands bound to the Src SH2 domain. This novel binding mode is being used in guiding future design efforts.

Introduction

Cellular signal transduction pathways for many growth factors, cytokines, and hormones proceed through a series of phosphorylating and dephosphorylating events.[1,2] Src homology 2 (SH2) domains,[3−8] which are found in numerous signal transduction proteins, play a pivotal role in such cascades. They bind phosphorylated tyrosine (pTyr) containing protein sequences, thus affording molecular association and translocation. Selective blockade of the binding sites of SH2 domains may alter the signaling process and potentially impact the cellular response and, in addition, may help to further elucidate complex signaling pathways. This biological information, coupled with the availability of X-ray and NMR structural data for SH2 domains,[9−13] project SH2 domains as prime targets for ligand design. The SH2 domain of the nonreceptor Src tyrosine kinase has been reported to bind to the focal adhesion kinase (FAK)[14]

and the activated receptors of PDGF[15] and EGF.[16] Recent studies have indicated that Src SH2 ligands are likely to be effective as therapeutic agents in controlling aberrant signaling and potentially treating breast and colon carcinomas.[17] Furthermore, this class of ligands has been implicated in the treatment of osteoporosis based on its antiresorptive activity in osteoclasts.[18] Therefore, structure-based *de novo* design of Src SH2 domain ligands has been a focus of our research efforts.

SH2 domains are relatively small protein units, composed of approximately 100 amino acid residues. As a family, they adopt a general fold that consists of a central beta sheet core flanked by two α-helices.[9,19] Two recently reported X-ray structures for the c-Src[20,21] and Hck[22] approximate full-length kinases reveal that this topology is retained in the more complete structures. An X-ray crystal structure of the v-Src SH2 domain bound with a high-affinity 11-residue peptide (11-mer, **1**, Table 1),[11] which contains the cognate sequence, pTyr-Glu-Glu-Ile,[23] has provided critical information regarding the intermolecular interactions in the binding site (Figure 1). The 11-mer binds

---

(1) Liu, D.; Wang, L.-H. *J. Biomed. Sci.* **1994**, *1*, 65.

(2) Walton, K. M.; Dixon, J. E. *Annu. Rev. Biochem.* **1993**, *62*, 101.

(3) Sadowski, I.; Stone, J. C.; Pawson, T. *Mol. Cell. Biol.* **1986**, *6*, 4396.

(4) Cohen, G. G.; Ren, R.; Baltimore, D. *Cell* **1995**, *80*, 237.

(5) Beattie, J. *Cell. Signal.* **1996**, *8*, 75.

(6) Pawson, T.; Schlessinger, J. *Curr. Biol.* **1993**, *3*, 434.

(7) Pawson, T. *Nature* **1994**, *373*, 573.

(8) Schlessinger, J. *Curr. Opin. Genet. Dev.* **1994**, *4*, 25.

(9) Kuriyan, J.; Cowburn, D. *Curr. Opin. Struct. Biol.* **1993**, *3*, 828.

(10) Waksman, G.; Komonos, D.; Robertson, S. C.; Pant, N.; Baltimore, D.; Birge, R. B.; Cowburn, D.; Hanafusa, H.; Mayer, B. J.; Overduin, M.; Resh, M. D.; Rios, C. B.; Silverman, L.; Kuriyan, J. *Nature* **1992**, *358*, 646.

(11) Waksman, G.; Shoelson, S. E.; Pant, N.; Cowburn, D.; Kuriyan, J. *Cell* **1993**, *72*, 779.

(12) Xu, R. X.; Word, J. M.; Davis, D. G.; Rink, M. J.; Willard, D. H., Jr.; Gampe, R. T., Jr. *Biochemistry* **1995**, *34*, 2107.

(13) A Src SH2 domain structural paper was recently reported by Glaxo Wellcome, Inc.: Charifson, P. S.; Shewchuk, L. M.; Rocque, W.; Hummel, C. W.; Jordan, S. R.; Mohr, C.; Pacofsky, G. J.; Peel, M. R.; Rodriguez, M.; Sternbach, D. D.; Consler, T. G. *Biochemistry* **1997**, *36*, 6283.

(14) Xing, Z.; Chen, H.-C.; Nowlen, J. K.; Taylor, S. J.; Shalloway, D.; Guan, J.-L. *Mol. Biol. Cell* **1994**, *5*, 413.

(15) Mori, S.; Ronnstrand, L.; Yokote, K.; Engstrom, A.; Courtneidge, S. A.; Claesson-Welsh, L.; Heldin, C.-H. *EMBO J.* **1993**, *12*, 2257.

(16) Luttrell, D. K.; Lee, A.; Lansing, T. J.; Crosby, R. M.; Jung, K. D.; Willard, D.; Luther, M.; Rodriguez, M.; Berman, J.; Gilmer, T. M. *Proc. Natl. Acad. Sci. U.S.A.* **1994**, *91*, 83.

(17) Boerner, R. J.; Kassel, D. B.; Barker, S. C.; Ellis, B.; Delacy, P.; Knight, W. B. *Biochemistry* **1996**, *35*, 9519.

(18) Dunnington, D.; Votta, B.; Hand, A.; Appelbaum, E.; Jones, C.; Prichett, W.; Holt, D.; Yamashita, D.; Gowen, M. Annual Meeting of the American Society of Bone and Mineral Research, September 8−11, 1996 Seattle, WA; Poster no. 395.

(19) The secondary structures are labeled A, B, C, etc., according to their location in the primary sequence, e.g., the first β-strand in the sequence is designated "βA", the second β-strand is designated "βB", etc., the first α-helix in the sequence is designated "αA", and the second α-helix is designated "αB". The loops are designated by the letters of the secondary structures they connect, e.g., the BC loop connects B β-strand and C β-strand.

(20) Cellular and viral forms of the Src gene are designated c-Src and v-Src, respectively. For a review, see: Brown, M. T.; Cooper, J. A. *Biochim. Biophys. Acta* **1996**, *1287*, 121.

(21) Xu, W.; Harrison, S. C.; Eck, M. J. *Nature* **1997**, *385*, 595.

(22) Sicheri, F.; Moarefi, I.; Kuriyan, J. *Nature* **1997**, *385*, 602.

Table 1. Binding Affinities of Peptide Ligands to the Src SH2 Domain

compd no.	analog	IC_{50} (μM)
1	Glu-Pro-Gln-pTyr-Glu-Glu-Ile-Pro-Ile-Tyr-Leu	0.8
2	Ac-pTyr-Glu-Glu-Ile-NH$_2$	4.3
3	Ac-pTyr-Glu-D-Hcy-NH$_2$[a]	1.8

[a] Hcy = homocyclohexylalanine.
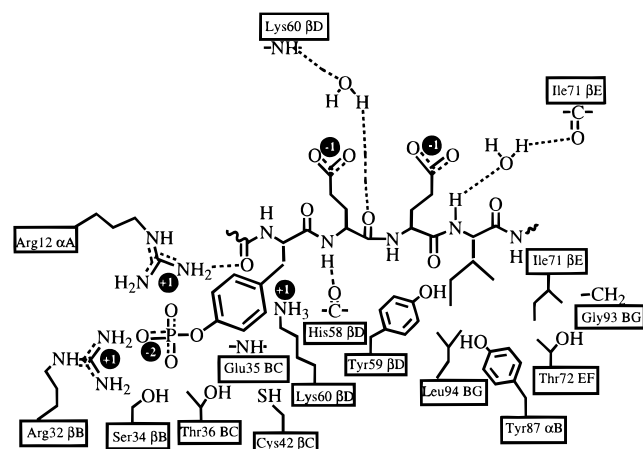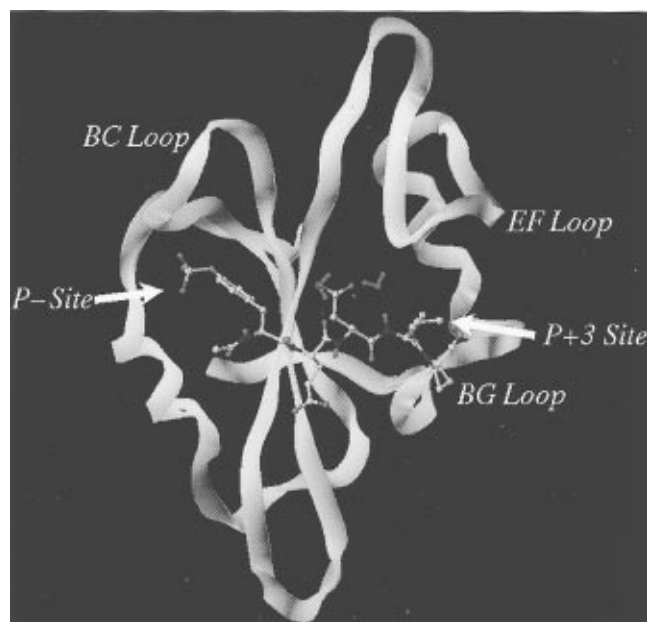
Figure 1. (a) A ribbon representation of the Src SH2 domain from the X-ray structure bound with the 11-mer[11] is shown in yellow. The 11-mer is truncated to a 5-mer (colored by atom type), which contains the cognate sequence pTyr-Glu-Glu-Ile. Two water molecules, which mediate interactions between the P+1[26] Glu(CO) and Lys60(NH), and the P+3 Ile(NH) and Ile71(CO) are shown in green. Arrows point to the pTyr (P-Site) and the Ile (P+3) binding sites. The BC loop, which forms in part the P-site and the EF and BG loops, which form in part the P+3 site are labeled. (b) Schematic of key residues that interact with the cognate sequence of the 11mer in the Src SH2 domain binding site.[11,19]

with an $IC_{50} = 0.8$ μM, although, the binding primarily involves the cognate sequence in the peptide, as is clearly evident in the X-ray structure and in the affinity ($IC_{50} = 4.3$ μM)[24,25] of the Ac-pTyr-Glu-Glu-Ile-NH$_2$ peptide (**2**, Table 1). A positively

charged pocket, the so-called P-site,[26] which binds the pTyr residue is formed in part by Arg12, Arg32, and Lys60. Additional polar interactions exist between the phosphate group and other P-site residues, namely Glu35 and Thr36 located in the BC loop[19] and Ser34 in the B β-strand (Figure 1). Thus, the phosphophenyl group engages in multiple intermolecular contacts with the surrounding protein residues. The ligand P+1 Glu(NH) forms a hydrogen bond with His58(CO), however, the P+1 and P+2 side chains only participate in surface interactions with the protein. The P+1 Glu(CO) and P+3 Ile(NH) form hydrogen bonds with bound water molecules, which in turn bind to Lys60(NH) and Ile71(CO), respectively. The side chain of P+3 Ile occupies a pocket formed by the EF and BG loops (Figure 1). Together, the pTyr and the P+3 Ile represent the major points of contact with the domain and promote essentially a two-point attachment effect in binding. In our laboratories, using a peptidomimetic approach, we have designed a pTyr tripeptide series that satisfies these two binding sites, while affording enhanced affinity relative to the tetramer (**3**, Table 1).[24,27] However, due to the shortcomings related to bioavailability that generally arise with peptide-like analogs,[28,29] we have applied structure-based design methodology toward the *de novo* discovery of small molecule, nonpeptide ligands.

Results and Discussion

Our initial strategy for the design of a Src SH2 domain ligand was to satisfy the P and P+3 pockets and bridge these binding moieties using a nonpeptide template or linker. In the cognate sequence, the side chains of the two central Glu residues lie on the protein surface, suggesting that the contribution of the charged carboxylates to binding was nonessential. Therefore, we targeted a template with no formal charge. In addition, we directed our design toward the displacement of water molecules that mediate the interactions of the P+1 and P+3 residues in the 11-mer, thus enhancing the entropic contribution to binding. Toward this end, the template segment was designed to bind directly to Lys60(NH) and Ile71(CO) and became the critical challenge in this research strategy.

The X-ray crystal structure of the Src SH2 domain bound with the 11-mer[11] was used as the starting structure for the design process. The phenyl phosphate group in pTyr appeared to be tightly bound in the P-site. The Src SH2 domain X-ray structures bound with lower affinity peptides also revealed these comprehensive internal interactions that clearly delineated the structural boundaries of the pTyr binding pocket.[10] For this reason, the phosphophenyl coordinates from the 11-mer complex were used as an "anchoring" group from which the remainder of the nonpeptide ligand was modeled and manually docked in the binding site. The premise was to incorporate a fairly rigid group as the bridging template, which would have the capability

(23) Songyang, Z.; Schoelson, S. E.; Chaudhuri, M.; Gish, G.; Pawson, T.; Haser, W. G.; King, F.; Roberts, T.; Ratnofsky, S.; Lechleider, R. J.; Neel, B. G.; Birge, R. B.; Fajardo, J. E.; Chou, M. M.; Hanafusa, H.; Schaffhausen, B.; Cantley, L. C. *Cell* **1993**, *72*, 767.

(24) Plummer, M. S.; Lunney, E. A.; Para, K. S.; Vara Prasad, J. V. N.; Shahripour, A.; Singh, J.; Stankovic, C. J.; Humblet, C.; Fergus, J. H.; Marks, J. S.; Sawyer, T. K. *Drug Des. Disc.* **1996**, *13*, 75.

(25) The tetrapeptide was also reported by Glaxo Research Institute: Gilmer, T.; Rodriguez, M.; Jordan, S.; Crosby, R.; Alligood, K.; Green, M.; Kimery M.; Wagner, C.; Kinder, D.; Charifson, P.; Hassell, A. M.; Willard, D.; Luther, M.; Rusnak, D.; Sternbach, D. D.; Mehrotra, M.; Peel, M.; Shampine, L.; Davis, R.; Robbins, J.; Patel, I. R.; Kassel, D.; Burkhart, W.; Moyer, M.; Bradshaw, T.; Berman, J. *J. Biol. Chem.* **1994**, *269*, 31711.

(26) Nomenclature for binding sites designates P for pTyr site. Residues N-terminal to P are P-1, P-2, etc.; residues C-terminal to P are P+1, P+2, etc.

(27) Related tripeptides were also reported by Glaxo Wellcome Research Institute: Rodriguez, M.; Crosby, R.; Alligood, K.; Gilmer, T.; Berman, J. *Lett. Pept. Sci.* **1995**, *2*, 1.

(28) Verhoef, J. C.; Bodde, H. E.; de Boer, A. G.; Bouwstra, J. A.; Junginger, H. E.; Merkus, F. W.; Breimer, D. D. *Eur. J. Drug Metab. Pharmacokinet.* **1990**, *15*, 83.

(29) Navia, M. A.; Chaturvedi, P. R. *Drug Discov. Today* **1996**, *1*, 179.
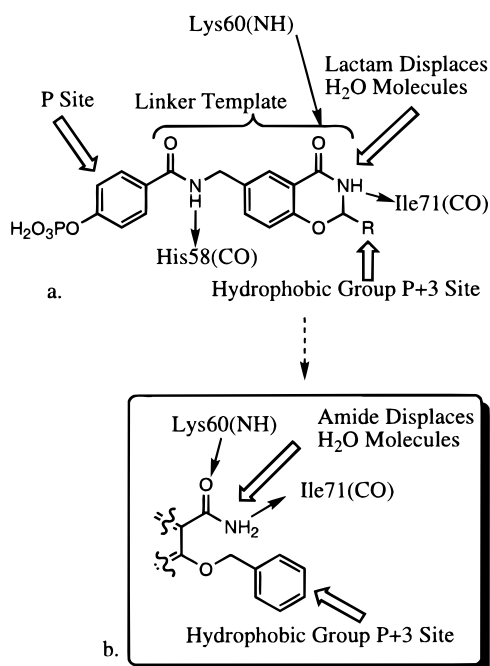
Figure 2. (a) Interactions of the proposed benzoxazinone Src SH2 domain ligand. (b) Interactions of the modified "ring-opened" form.

of forming hydrogen bonds directly with Lys60 and Ile71, as described above. An appropriately functionalized ring system would meet these requirements. A search of the Cambridge Crystallographic Database[30] suggested that a benzoxazinone bicycle (Figure 2a) was a potential candidate for the linking template. Using molecular modeling, the benzoxazinone moiety was attached at C-7 through a methyleneamide group to the *para* position of the phosphophenyl "anchor". The amide NH was positioned to form a hydrogen bond with His58(CO), thus mimicking the interaction observed with the P+1 NH in the 11-mer. The benzoxazinone ring was oriented with the ring oxygen pointed to the Lys60(NH) and the lactam NH directed toward Ile71(CO). Unfortunately, with this orientation, the benzoxazinone ring could not be suitably substituted with groups that would reach the P+3 site. Further analysis showed that by attachment of the bicyclic system at C-6 and alteration of the puckering of the benzoxazinone ring, the group could then be oriented such that the lactam could serve as both an acceptor with Lys60(NH) and a donor to Ile71(CO). Substituting a hydrophobic group at the C-2 position of the benzoxazinone ring afforded binding in the P+3 pocket (Figure 2a), and thus, both the P and P+3 sites would be occupied by the analog. After ligand minimization and refined docking, the modeled structure retained the desired interactions and was considered a reasonable target to pursue; however, the synthetic feasibility became a concern. Rather than abandon the design concept, a "ring-opened" form of the bicyclic system was modeled. Specifically, the benzoxazinone ring system was modified to a phenyl group substituted relative to the methyleneamide by a carboxamide in the *meta* position and by an ether linkage to a hydrophobic group in the *para* position (Figure 2b). Molecular modeling indicated that the *meta* amide group could satisfy the polar interactions with Lys60 and possibly Ile71 and that the hydrophobic ether side chain could bind in the P+3 pocket (Figure 3).

The first compound in the series to be synthesized was the *O*-benzyl derivative **4**, which bound to the Src SH2 domain construct with an IC$_{50}$ = 9.7 μM (Table 2). This initial result was encouraging and supported the design strategy. While crystallographic studies were being initiated, the model of the bound ligand guided further molecular design efforts to increase the binding affinity of this small, achiral nonpeptide. We realized an improved potency by modifying the hydrophobic group of the ether side chain to increase the interactions at the P+3 site. Replacement of the phenyl group with either a *m,m*-dimethylphenyl side chain (Figure 3) or a cyclohexyl ring resulted in increased affinities as is seen with **5** and **6** (Table 2). These results lent additional support that our analogs were occupying the P+3 pocket. Other P+3 substituents were investigated but exhibited no enhancement in activity, e.g., **7**. In this case, the affinity improvement expected from probing more deeply into the P+3 pocket with the extended alkyl chain was most likely offset by an unfavorable entropic effect. Conversely, removal of the alkyl group as in **8** or total deletion of the *para* substituent as in **9**, abolished activity (Table 2).

The importance of the *meta*-substituted amide functionality on the phenyl ring in the bridging template was also quite evident, since any modification at this site, e.g., *N*-methylamide (**10**), produced in a drop in potency (Table 3). Modeling indicated that the *N*-methylation might alter the binding mode to some degree due to the close contact with either Lys60 or Ile71. The analog without a *meta* substituent was inactive (**11**). These findings strongly suggested that the amide functionality was involved in a favorable polar interaction with the protein as was predicted in the modeling.

Analysis of the model indicated that substituting the methylene moiety in the linker with a methyl group to provide the *S* configuration would improve van der Waals contact with the protein. In addition, the entropic effect on the ligand might enhance the affinity. The methylated derivative was synthesized in the cyclohexyl series as a racemate (**12**) and indicated improved potency for the desired enantiomer (Table 3).

Modification of the phenyl ring in the P-site was tolerated, although improved potency was not realized, as illustrated by **13** (Table 3). The presence of the methyl substituents *ortho* to the phosphate in **13** might, however, improve the stability of this labile group. Another approach that addresses the phosphate stability[31] and has been applied successfully in the peptide series[32] involves replacing the phosphate of pTyr with a phosphonodifluoromethyl group, i.e., Phe-(*p*-CF$_2$PO$_3$H$_2$) or F$_2$Pmp. The incorporation of this pTyr mimetic in the original 11-mer, **1**, resulted in a 7-fold drop in potency (data not shown). In the *de novo* cyclohexyl series, the phosphonodifluoromethyl substitution effected a comparable reduction in affinity (**14**, Table 3). Finally, the phosphate was not successfully mimicked by a *m-*, *p*-dicarboxylate substitution of the P-site phenyl ring (**15**), and total deletion of an acidic functionality at this site also resulted in an inactive analog (**16**).

Crystals of **5** complexed with Src SH2 domain were obtained, and the X-ray data were collected. Two solutions were determined, corresponding to the two independent Src SH2 molecules in the asymmetric unit. The conformation of the bound inhibitor is similar in the two Src SH2 molecules. The nearly linear ligand binds in the phosphopeptide binding site in

(30) (a) Allen, F. H.; Bellard, S.; Brice, M. D.; Cartwright, B. A.; Doubleday, A.; Higgs, H.; Hummelink, T.; Hummelink-Peters, B. G.; Kennard, O.; Motherwell, W. D. S.; Rodgers, J. R.; Watson, D. G. *Acta Crystallogr.* **1979**, *B35*, 2331. (b) Allen, F. H.; Kennard, O.; Taylor, R. *Acc. Chem. Res.* **1983** *16*, 146.

(31) Burke, T. R., Jr.; Smyth, M. S.; Otaka, A.; Nomizu, M.; Roller, P. P.; Wolf, G.; Case, R.; Shoelson, S. E. *Biochemistry* **1994**, *33*, 6490.

(32) Shahripour, A.; Plummer, M. S.; Lunney, E. A.; Vara Prasad, J. V. N.; Singh, J.; Para, K. S.; Stankovic, C. J.; Eaton, S. R.; Rubin, J. R.; Pavlovsky, A. G.; Humblet, C.; Fergus, J. H.; Marks, J. S.; Decker, S. J.; Hererra, R.; Hubbell, S.; Saltiel, A. R.; Sawyer, T. K. *Peptides: Chemistry, Structure and Biology*; Mayflower Scientific Ltd.: West Midlands, England, 1995; pp 394−396.
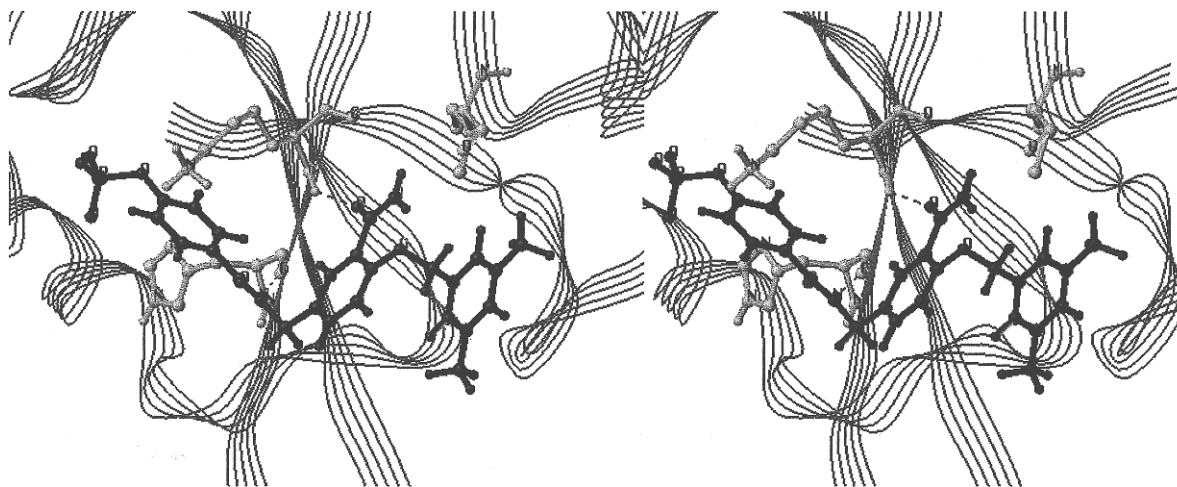
Figure 3. Stereoview: **5** (black) docked in the Src SH2 domain, which is represented in part as a ribbon structure. His58, Lys60, and Ile71 in the protein are shown in gray. The phosphophenyl moiety is oriented in the P-site and the dimethylphenyl group is positioned in the P+3[26] site. Hydrogen bonds are shown between the amide NH attached to the phosphophenyl group and His58(CO) and between the carboxamide CO substituted on the linker phenyl group and Lys60(NH).

Table 2. Binding Affinities of *De Novo* Analogs Modified at the P+3 Site[26]

compd no.	analog	IC$_{50}$ (μM)
4		9.7
5		6.6
6		6.5
7		~20
8		>100
9		>100

Table 3. Binding Affinities of *De Novo* Analogs

compd no.	analog	IC$_{50}$ (μM)
6		6.5
10		~30
11		>100
12		5.6
13		12.5
14		~50
15		>100
16		>100

each molecule and engages in the interactions proposed in the design concept (Figure 4). These include the primary two-point interaction sites: the phosphophenyl in the P-site and the dimethylphenyl in the P+3 pocket. In addition, the crystal structure analysis shows that two key polar contacts are also attained. First, the NH of the amide directly attached to the phosphophenyl ring is a hydrogen-bond donor to His58(CO), thus mimicking the interaction observed with the P+1 NH in the 11-mer. Second, and more interestingly, the carboxamide

substituted on the phenyl in the linker template displaces water molecules found in the 11-mer X-ray structure and binds directly to Lys60(NH). The carboxamide NH2 is oriented too far from Ile71 for a polar contact; however, the mediating water between the P+3 peptide residue and Ile71(CO) is displaced. Thus, the strategy of displacing bound water molecules is indeed suc-
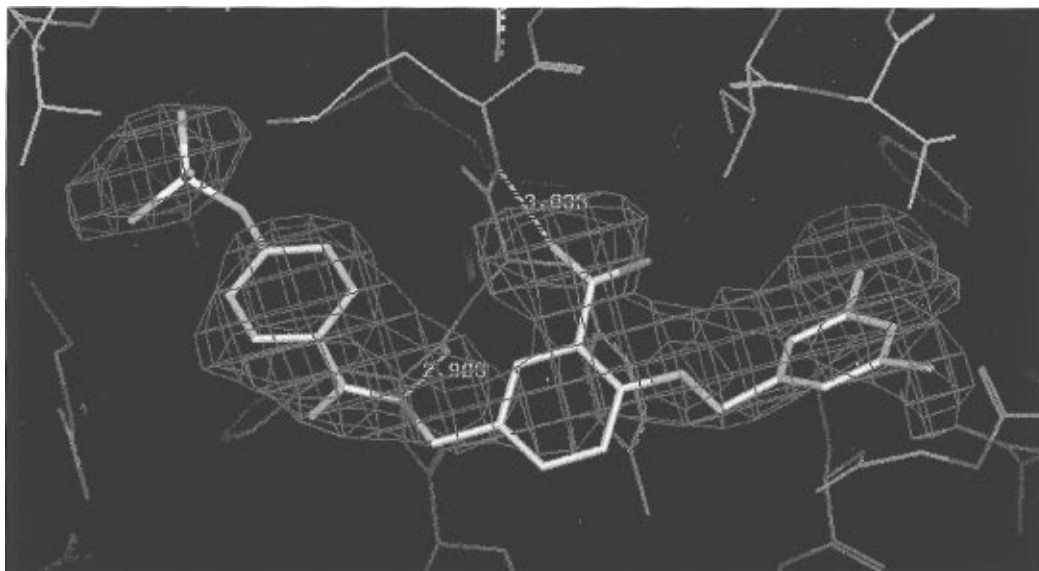
Figure 4. The refined structure of **5** (thick lines) bound to the Src SH2 domain (molecule 1). The hydrogen bond between the ligand amide attached to the phosphophenyl ring and His58(CO) and the one between the carboxamide on the template phenyl and Lys60(NH) are shown. The caged electron density (cyan) is from the original $F_o - F_c$ difference electron density map. The map is contoured at 1.5 times the standard deviation of the map.
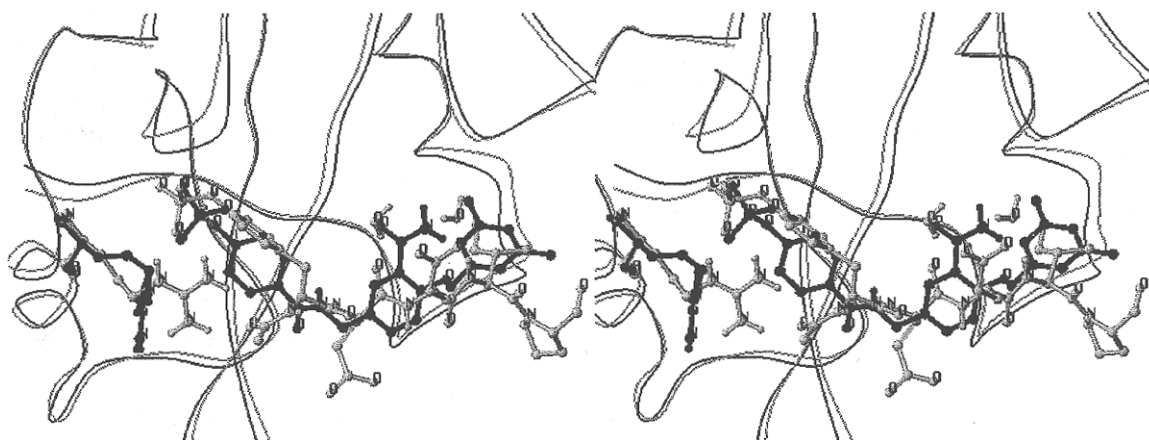

Figure 5. Stereoview: Overlay of the X-ray structures of **5** (black ligand) and the truncated 11-mer (gray ligand) bound to Src SH2 domain. A ribbon representation for each protein structure is shown in part along with Arg12 (black for the complex with **5**, gray for the 11-mer structure). Two water molecules, which mediate interactions between the P+1[26] Glu(CO) and Lys60(NH) and the P+3 Ile(NH) and Ile71(CO) in the 11-mer structure are shown in gray. The overlay contrasts the orientations of the phosphophenyl groups in the P-site and shows the corresponding rotamers for Arg12. The shift in the BC loop at the P-site is also shown. The carboxamide substituted on the linker phenyl group in **5** is shown as displacing the two bound water molecules in the 11-mer structure. The dimethylphenyl group in **5** is positioned deeply in the P+3 site, which is occupied by the Ile in the 11-mer.

cessful with the ligand template interacting directly with the protein as rationally designed.

Although the key interactions between the ligand and the SH2 domain have been substantiated, the bound ligand conformation in the X-ray structure differs from that originally modeled. The reason for this contrast can be traced to the binding mode in the P-site. As has been described above, the coordinates for the phosphophenyl group from the 11-mer structure were used in modeling the *de novo* structures, and from this "anchor", the linker template and the hydrophobic moiety were built. However, the X-ray structure of the Src SH2 domain bound with **5** reveals that the phosphophenyl group binds significantly differently in the P pocket, such that the plane of the phenyl ring is oriented approximately 65° relative to that in the model and, thus, also the 11-mer X-ray structure (Figure 5). With the phosphophenyl orientation in **5**, Arg12 is forced to rotate away from the position observed in the Src SH2 domain X-ray structures bound with peptides (Figure 5). This results in a loss of the cationic/π interaction between the Arg12 guanidine group

and the phosphophenyl ring, although an ionic interaction remains between Arg12 and the phosphate group in one of the SH2 domain molecules. In addition, the positioning of the phosphate group in the X-ray structure with **5**, relative to that in the model, is shifted slightly toward the standard P+1 binding site. This results in the BC loop being drawn in more closely to the binding site to interact with phosphate group (Figure 5).

Since a binding mode for the phenylphosphate group significantly different from that observed in the Src SH2 domain X-ray structure bound with **5** was used in the ligand design, it is not surprising that the remainder of the ligand undertakes a different orientation to attain the targeted interactions. Specifically, variations are noted in the two torsion angles between the phosphophenyl amide group and the linker phenyl ring, and the torsion angle between the ether oxygen and the methylene group at the P+3 site. In addition, the dimethylphenyl group in the X-ray structure binds more deeply in the P+3 pocket, forming contacts with Tyr87. Conversely, the modeled conformer interacts more at the surface at this site.

It is clear from these experimental results that the complexity and multiplicity of binding, due in part to the dynamic nature of the phenomenon, should never be underestimated. Although the previous Src SH2 domain X-ray structures bound with peptide ligands revealed a distinct binding mode for the phenylphosphate moiety, the X-ray structure with **5** reveals that the phenylphosphate is capable of an altered binding mode at the P-site and the protein, in turn, adjusts to optimize the critical interactions. Indeed, the binding at the P+3 site might be considered the more conserved interaction of the two-point binding mode in going from the 11-mer peptide to the *de novo* series of ligands. These results promote molecular docking experiments, which are focused more on the structural information available for the shapes and properties of protein binding sites than on the particular binding modes of somewhat remotely related ligands. This approach would afford a more comprehensive analysis of potential binding orientations, although the accurate prediction of binding interactions would continue to remain a nontrivial task. These results also highlight the importance of the iterative aspect of structure-based design, wherein the determination of multiple, key, 3-dimensional complexes can refine the existing design strategy and possibly set new directions for future design efforts.

Conclusion

The insight gained from the X-ray structure of the Src SH2 domain bound with **5** is invaluable for future design efforts with this series. The original model provided us with a rational basis for the inception and initial advancement of this *de novo* design series. Since the key interactions predicted in the model were ultimately revealed in the X-ray structure, it is not surprising that the structure−activity relationships observed with the *de novo* analogs were in agreement with that proposed with the modeling. With the X-ray complex determination, the first cycle in the iterative structure-based design application is completed and the new information can now be used to guide the analog design to improved levels of potency. In addition, the novel binding at the P-site might be capitalized upon for designing new phosphate mimetics that are more conducive to cell penetration and increased bioavailability. The unique binding results heighten the potential of this novel and exceptional series that has already progressed dramatically from the original peptide ligand to a small molecule structure with significant potency in binding to the Src SH2 domain.

Experimental Section

Molecular Modeling. Modeling was carried out using the SYBYL molecular modeling software,[33] the SH2 domain X-ray structure bound with the 11-mer,[11] and a Silicon Graphics workstation. The coordinates for the phosphophenyl group from the 11-mer ligand were used as an "anchor" from which the *de novo* structures were built and manually docked in the binding site. Specifically, polar interactions were targeted with His58, Lys60, and Ile71. The latter two contacts result in the displacement of water molecules present in the 11-mer X-ray structure. A hydrophobic group was positioned in the P+3 pocket. Energy minimizations were carried out using the Tripos force field. Compound **6** was finally minimized in the binding site with the protein, the phosphophenyl, and the cyclohexyl groups aggregated and employing electrostatics. KOLL_UNI charges were used for the protein, and ESP[34] charges were used for the ligand. The docking of cyclohexyl group in

the minimized structure was then manually refined by positioning the ring slightly deeper in the P+3 site. Compound **5** was modeled using this final structure of **6**. The cyclohexyl group was replaced with the dimethylphenyl ring, which was oriented in the P+3 pocket. The ligand structure was minimized without electrostatics, aggregating all but the terminal substituted ring.

The puckering of the benzoxazinone ring system extracted from the Cambridge Crystallographic Database[30] was altered by reflecting oxazinone atoms through a plane defined by the six ring atoms of the oxazinone ring.

Crystallization. Crystals of **5** complexed with Src SH2 domain were obtained at room temperature by the hanging-drop vapor diffusion method. Soluble Src SH2-GST fusion protein had been purified on a glutathione sepharose column and cleaved with thrombin. The cleaved Src SH2 domain was purified by glutathione sepharose and size exclusion chromatography. A 4 μL aliquot of protein solution (50 mg/mL Src SH2 protein, 0.1 M NaCl, 0.01 M Tris, pH 7.0) was combined with 2 μL of **5** solution (10 mM) and 4 μL of reservoir solution (32% PEG 6000, 0.1 M MES, pH 6.0) and allowed to equilibrate against 1 mL of reservoir solution. Rod-shaped crystals of the complex (0.1 mm × 0.1 mm × 0.4 mm) appeared after several weeks.

Data Collection. The X-ray diffraction data to 2.5 Å resolution were collected on the Src SH2 domain complexed with **5** using a MarResearch Image Plate X-ray detector and a Rigaku Ru-200B rotating anode X-ray generator operating at 50 kV and 120 ma. The crystals of the complex are monoclinic, space group $P2_1$, with unit cell dimensions $a = 27.81$ Å, $b = 55.26$ Å, $c = 65.98$ Å and $\beta = 98.69°$, with two independent Src SH2 molecules in the asymmetric unit. A total of 5695 reflections (out of a possible 6985) with $I/\sigma(I) \geq 2.0$ were measured to 2.5 Å resolution with a symmetry R-factor of 8.17% on intensity and an average redundancy of 1.8.

Structure Determination and Refinement. The structure was solved using the AmoRe molecular replacement and refinement programs[35] together with the refined coordinates of the phosphate complex of Src SH2 domain.[11] Two solutions were determined, corresponding to the two independent Src SH2 molecules in the asymmetric unit. The solutions have a combined correlation coefficient of 0.642 and a crystallographic R-factor of 0.349. The structure was further refined using XPLOR.[36] Difference electron density maps using data to 2.5 Å resolution revealed the position and conformation of **5** in each of the two independent Src SH2 molecules. The full structure including two Src SH2 domains and two bound ligands, but excluding water molecules, was refined using XPLOR to a final R-factor of 0.235 using data from 25.0 to 2.5 Å resolution.

IC$_{50}$ Determinations. The compounds were tested using an assay in which the binding of ^{125}I-**1** to the GST-Src SH2 domain fusion protein was performed in 20 mM Tris pH 7.5, 150 mM NaCl, 5 mM EDTA, and 0.1% NP-40. Assay additions resulted in Src SH2 fusion protein-glutathione sepharose bead complex, 2.8 nM ^{125}I-**1**, and 2% DMSO test compound at concentrations ranging from 0.1 to 100 μM. Binding was carried at room temperature for 20 min while continuously inverting the plate. Bound ^{125}I-**1** was separated from free by vacuum filtration and washing two times with 100 μL of assay buffer/well. The remaining radioactivity was determined by scintillation counting. All measurements were determined in duplicate.

Supporting Information Available: Complete experimental details for compounds **4−16** (11 pages). See any current masthead page for ordering and Internet access instructions.

(33) SYBYL Software Program (Versions 6); Tripos Inc., 1699 S. Hanley Road, St. Louis, MO 63144-2913.

(34) Besler, B. H.; Merz, K. M., Jr.; Kollman, P. A. *J. Comput. Chem.* **1990**, *11*, 431.

(35) Navaza, J. *Acta Crystallogr.* **1994**, *A50*, 157.

(36) X-PLOR, Version 3.1; A System for X-ray Crystallography and NMR; Axel T. Brunger; Yale University Press: New Haven, CT, 1992.